A Scanning Thermal Microscopy System with a Temperature Dithering, Servo-Controlled Interface Circuit

Joohyung Lee[1] and Yogesh B. Gianchandani[1,2]

[1]ECE Department, University of Wisconsin, Madison, WI 53706, USA
[2]EECS Department, University of Michigan, Ann Arbor, MI 48109, USA

ABSTRACT

This paper describes a thermal imaging system which includes a customized micromachined thermal probe and circuit interface for a scanning microscopy instrument. The probe shank is made from polyimide for mechanical compliance and high thermal isolation, and has a thin-film metal tip of ≈50 nm in diameter. The circuit provides closed-loop control of the tip temperature and also permits it to be dithered, facilitating scanning microcalorimetry applications. This paper explains system design and optimization including both electrical and thermal analyses. Sample scans of patterned photoresist demonstrate noise-limited resolution of 29 pW/K in thermal conductance. Applications of the thermal imager extend from ULSI lithography research to biological diagnostics.

I. INTRODUCTION

In the past decade, scanning microscopy using thermally-sensitive probes has been applied to a variety of applications, ranging from ULSI lithography research to cellular diagnostics in biochemistry [Oc96, Li02]. Thermal probes have also been employed for data storage and other applications [Ve00, Le00, Ma99]. These are generally made from dielectric thin films on a silicon substrate, and use a metal or semiconductor film bolometer for sensing the tip temperature. Other approaches that use more involved micromachining methods have also been reported [Gi97]. A commercially available probe uses a narrow gauge wire bent into a V-shape to form a self-supporting resistor. However, for many applications, thermal probes must have very low mechanical spring constants to prevent damage to soft samples. In addition, for many applications they must have very high thermal isolation to minimize the thermal load presented to the sample. Both of these needs can be met by the use of a polymer for the probe shank. Furthermore, thermal and mechanical design challenges must be considered in conjunction with the interface circuit for best performance of the overall system.

In a frequently used microscopy technique, the scanning tip is mechanically dithered so that the sample spacing is modulated at a known frequency. This is akin to chopping the signal, which permits the detection to be phase locked to the dither, improving the overall signal-to-noise ratio. In the context of thermal microscopy, this also permits thermal capacitance measurement. However, with ultracompliant probes, the mechanical spring constant is far too low to permit physical dithering. The alternative is to dither the bias current in the bolometer, thereby placing the burden on the interface circuit. Furthermore, the very high thermal resistance of the probe shank, designed to minimize thermal loading of the sample, has the impact of reducing the thermal bandwidth of the probe below 1 KHz. This increases the susceptibility of the pick-off to flicker noise and further raises the burden on the circuit.

This paper describes a thermal imaging system (Fig. 1) which uses a customized micromachined bolometer probe and circuit interface to a commercial scanning microscopy instrument (TopoMetrix™ SPMLab v.3.06). The bias current in the bolometer can be controlled to operate the scan at a fixed temperature. The interface also provides electronic dithering of the tip temperature. Its design includes consideration of thermal and electrical interactions between the probe and circuit components based on MatLab™ modeling of the overall system. The functionality of the system is demonstrated with both microcalorimetric and imaging applications of patterned photoresist and calibration materials. To further evaluate the operation of the circuit, nodal measurements taken during a practical scan (not in a test mode), and are presented along with the scanned image obtained.

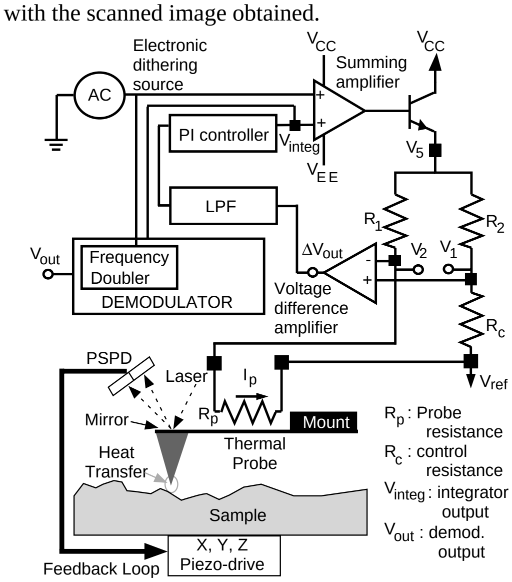

Fig. 1: The overall system configuration of the custom probe and circuit which interface with a commercial instrument.

II. SYSTEM DESCRIPTION

A. Sensor Element

The scanning thermal probe is fabricated on a Si substrate using a 7 mask process similar to those described in [Li00, Li01]. A metal thin film bolometer is sandwiched between two layers of polyimide that form a cantilever (Fig. 2). At one end of the cantilever the Ni thin film protrudes through an opening in lower polyimide layer, where it is molded into a pyramidal tip by a notch that was anisotropically wet-etched into the substrate. A tip diameter of ≈50 nm is achieved by sharpening the notch by anisotropic thermal oxidation. The tip and a portion of the probe shank are then released from the substrate by etching an underlying sacrificial layer. The released length is then folded over to extend past the die edge for clearance, and held in place by a thermo-compression bond across a thin film of Au which is deposited as the final layer on top of the polyimide. This film also serves as a mirror to permit use of the probe for AFM. The entire fabrication process is performed below 350°C, and is compatible with post-CMOS processing to accommodate the possible integration of an interface circuit. Typical dimensions of the probes after assembly are 250 µm length, 50 μm width, and 3 μm thickness, which result in a mechanical spring constant of 0.08 N/m, which is upto 100× below commercial probes. The bolometer, which has Cr/Ni at the tip and Cr/Au leads, is ≈45 Ω.

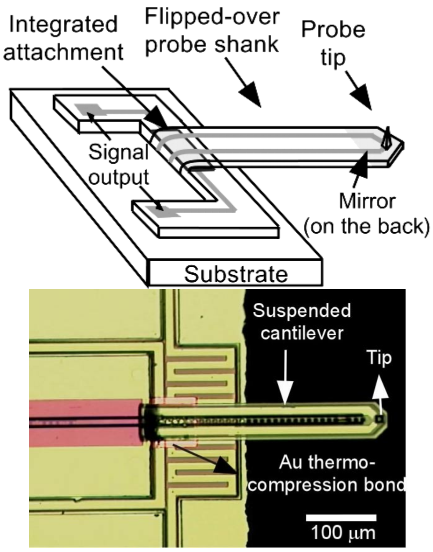

Fig. 2: Schematic and optical micrograph of a fabricated probe.

B. Interface Circuit

The bolometer readout is through a Wheatstone bridge, which is commonly used for piezoresistive pressure sensors, strain gauges, etc. It is well suited for microfabrication and allows a differential measurement that offers a higher common-mode noise rejection than a single-element measurement. Historically, the conversion of bridge resistance to current or voltage for readout has suffered from non-linearity and restricted dynamic range [Yo00]. Additionally, in DC mode the signal is subject not only to thermal noise from the resistor bridge, but also 1/f flicker noise from the electronics. To overcome these challenges, many efforts have been made to convert resistance variation to frequency [Mo95, Hu87, Gi76], to duty cycle/time [Ci90, Go93], and to both of them [Fe97]. Some require components such as a pulsed bridge supply current, or an input amplifier with very low offset and drift [Gi76]. Furthermore, these approaches are constrained by switching delays causing non-linearity between frequency (or pulse width) and resistance change, are expensive to implement, and most importantly cannot be applied directly to operating the microbolometer or anemometer in a constant temperature mode.

The system used in this effort (Fig. 1) utilizes two separate feedback loops: electrical and optomechanical. As the probe (Fig. 2) scans the sample surface, topography is mapped by detecting the laser signal reflected off a mirror located near the tip and using this in a mechanical feedback loop to maintain constant contact force. Since variations in heat loss through the probe tip cause variations in the probe resistance, this quantity maps the temperature or thermal conductance of the sample.

When both a DC and an AC signal (at ω_o) are applied to the bridge (Fig. 1), the bolometer is modulated by the square of $V_{DC}+V_{AC}\cos(\omega_o t+\theta)$, and its resistance changes proportional to:

$$\Delta R_p \propto V_{DC}^2+2V_{DC}V_{AC}\cos(\omega_o t+\theta) + V_{AC}^2\cos^2(\omega_o t+\theta) \qquad (1)$$

Therefore, bolometer resistance is approximately represented as:

$$R_p \approx R_{pDC} + R_{pAC}\cos(\omega_o t+\theta) \textit{ if } V_{AC}^2 << 2\cdot V_{DC}\cdot V_{AC} \qquad (2)$$

making ω_o the dominant resistance-modulation frequency. The output of the bridge voltage difference amplifier is:

$$\Delta V_{out}=0.5\cdot I_{AC}R_{pAC}\cos(2\omega_o t+\theta)+ I_{DC}R_{pAC}\cos(\omega_o t+\theta) \qquad (3)$$

If the $2\omega_o$ term (second harmonic) of the voltage-modulation frequency is selected, the impact of 1/f flicker noise can be reduced. In addition, better signal-to-noise ratio is expected as I_{AC} becomes high to a certain extent. In the selected implementation, V_{DC} was 5 V and V_{AC} was 0.8 V.

The interface circuit includes a PI controller (which is comprised of an integrator and an inverting amplifier), and a simple homodyne demodulator (Fig. 1), in which the input signal is multiplied by in-phase local oscillator and then low pass filtered (Fig. 3). The PI controller has integral gain of 10^4 and proportional gain of 1, showing settling time <10 msec. This demodulation technique (Method A) is applicable when phase change in the input signal is negligibly small compared to change in its magnitude. The Method A is simple to implement and does not have mismatch problems which are faced in quadrature homodyne demodulation (Method B). In Method B, in-phase (I signal) and quadrature (Q signal) signals are generated, low pass filtered, and root mean squared. Problems are caused by mismatches between the amplitude of I and Q signals and errors in the nominally 90° phase shift. Method A is consequently preferred. According to our previous investigations [Li01], the -3 dB frequency of thermal response of the probe is about 0.5 kHz with an open-loop interface circuit. It is somewhat higher with a closed loop interface circuit because external power is used to increase effective thermal conductance of the probe [Sa93]. Consequently, for this project a 1 kHz dither is selected, and scan speeds are set to provide a measured data bandwidth <50 Hz. The bridge output voltage is band pass filtered at the second harmonic 2 kHz, and multiplied by the frequency doubled output of the dither oscillator (Fig. 3). The phase of the local oscillator is synchronized with that of input carrier signal to avoid signal distortion. The final output is obtained by low pass filtering. The Q factor of band pass filter and -3 dB frequency of low pass filter are based on the dither frequency and data bandwidth, but adjusted for low frequency noise near the band edge of scan data. Bi-quad band pass filters and bi-quad low pass filters are used because of their excellent tuning features and good stability. The gain, quality factor, and salient frequencies of the filters can be independently controlled.

III. SYSTEM MODELING AND SIMULATION

The simulation of the whole sensing subsystem provides an understanding of the interaction between thermal behavior of the probe and electrical behavior of the interface circuit. It is accomplished using electrical parameters of the Simulink tool within MatLab™. Figure 4 shows the state diagram for the combined subsystem. Using this, it is demonstrated how the demodulator achieves noise reduction compared to a non-dithered DC closed loop interface circuit.

A challenge in modeling the subsystem is how to transform a thermal probe into electrical parameters. The dotted block in bottom left of Fig. 4 represents the thermal probe model. The three inputs shown are used to mimic the time variation of thermal conductance encountered during a scan of photoresist lines on a Si substrate. Thermal conductance changes smoothly in a real scan, but the variation should have a non-zero and finite bandwidth to test the circuit for signal distortion. The sum of these inputs is multiplied by the temperature bias of the tip to calculate the power variation in the probe. This variation, which would otherwise modulate the bolometer, is instantly compensated by the interface circuit which keeps the probe temperature constant.

An important optimization parameter for simulations is the ratio of V_{DC} to V_{AC} in eqn. (1). As V_{AC} increases, modulation of probe resistance by the second harmonic of applied power cannot be ignored. Additionally, simulations show that the PI controller loses its feedback control, even though the signal-to-noise at the output of demodulator becomes better in a certain range of V_{AC}. The probe temperature is supposed to be almost constant despite small AC temperature variations introduced for dither operation by the PI controller. However, as V_{AC} increases, power supplied by the AC component becomes comparable to DC power, causing the tip temperature to fluctuate significantly. Now the PI controller receives a significant AC signal in addition to the DC signal that is the differential output from the resistor bridge. The output of PI controller thus contains not only DC compensation power but also a significant amount of unnecessary AC power, which derails the PI feedback control. A low pass filter can be placed between bridge circuit and PI controller to avoid this problem. However, it is only useful when the dither frequency is much higher than bandwidth of the scan signal from the bridge. In the simulated system the mimicked signal at the input of the system contains frequency components at higher frequencies than the dithering signal.

Figure 4(a) represents a noiseless input to the system. When low frequency noise exists at 100 Hz, with a 20% variation in bolometer resistance the bridge output is deteriorated in the absence of electrical dithering (Fig. 4(b)). In contrast, the output of demodulator (Fig. 4(c)), which is used with electrical dithering, shows a much better signal-to-noise ratio. However, the output of demodulator can be distorted because high-frequency components of the input signal can be inadvertently screened by band pass filters with high quality factor. This motivates the use of the highest dither frequency (and thus a fast thermal response) to secure the maximum signal bandwidth.

IV. MEASUREMENT

Insets in Fig. 3 show frequency spectra at various circuit nodes taken while scanning a photoresist sample at a tip temperature of 45°C. Figure 3(a) shows that at the output of the bridge circuit, where the second harmonic contains the pursued power-modulated thermal signal, the amplitude ratio of the first harmonic to the second is 24.6, which is very close to the theoretical value of 25 obtained from eqn. (3). This demonstrates that the bandwidth of the thermal probe can be wider than 2 kHz and the 2 kHz-dithered signal is not distorted by thermal delay. Figure 3(b) shows that the band pass filtered signal has a dominant second harmonic. Filters with higher Q-factor can be used to suppress other harmonics, but could cause signal distortion due to reduced bandwidth. Figure 3(c) shows the output of the frequency doubling circuit, which serves as the local oscillator in demodulation. The dominant 2 kHz harmonic is obtained using a high Q-factor band pass filter. Figure 3(d) shows the multiplier output, where the DC component contains demodulated thermal signal. The output of the low pass filter shows that other harmonics can be effectively removed (Fig. 3(e)).

Figure 5 is a comparison of the thermal image with the topographic image obtained using closed loop interface circuit during measurements shown in Fig. 3. The sample was 350 nm thick, developed Shipley UV6™ photoresist, with a 1 µm pitch. The similarity between the two images is self-evident. The somewhat flatter top seen for the ridges in the thermal image is as expected because of the thermal diffusivity of the sample. According to a line scan across the photoresist patterns of Fig.5, the noise-limited minimum detectable thermal conductance change is ≈29 pW/K.

V. CONCLUSION

A scanning thermal imager with micromachined bolometer type probes and a custom interface circuit was described. Unified simulation of the transducer and circuit permits the components to be optimized together. The probe temperature can be precisely controlled by a PI controller while electrical dithering provides relative immunity to thermal bridge noise even for sub-µV low-frequency signals. Scanning thermal images obtained showed a high signal-to-noise ratio of 6 for 350nm UV photoresist in which the minimum detectable thermal conductance change was ≈29 pW/K.

ACKNOWLEDGEMENTS

This work was funded in part by the Semiconductor Research Corporation contract # 98-LP-452.005. Valuable discussions with Profs. F. Cerrina and P. Nealey, and Drs. M.-H. Li and R. Tate, all of UW-Madison, and Dr. L. Ocola of Argonne National Laboratory are gratefully acknowledged.

REFERENCES

[Ci90] A.Cichocki, R.Unbehauen, "Application of switched-capacitor self-oscillating circuits to the conversion of RLC parameters into a frequency or digital signal," *Sensors and Actuators A*, vol. 24, pp. 129-137, 1990

[Fe97] V.Ferrari, C.Ghidini, D.Marioli, A.Taroni, "Conditioning circuit for resistive sensors combining frequency and duty-cycle modulation on the same output signal," *Measurement Science & Technol.*, 8(7), pp. 827-9, '97

[Gi76] B.Gilbert, "A versatile monolithic voltage-to-frequency converter," *IEEE J. Solid-State Circuits*, SC-11(6), pp. 852-64, 1976

[Gi97] Y. Gianchandani, K. Najafi, "Scanning Thermal Profilers with Integrated Sensing and Actuation," *Transactions on Electron Devices*, 44 (11), Nov. 1997, pp. 1857-68

[Go93] F.M.L. van der Goes, P.C.De Jong, G.C.M.Meijer, "Concepts for accurate A/D converters for transducers," *Solid-State Sensors and Actuators (Transducers '93)*, Yokohama, Japan, 1993, pp. 331-4

[Hu87] J.H.Huijsing, G.A.Van Rossum, M.van der Lee, "Two-wire bridge-to-frequency converter," *J. Solid-State Circuits*, SC-22(3), pp. 343-9, 1987

[Le00] J. Lerchner, D. Caspary, G.Wolf, "Calorimetric detection of volatile organic compounds," *Sensors and Actuators B*, 70, pp. 57-66, 2000

[Li00] M.-H.Li, Y.B.Gianchandani, "Microcalorimetry applications of a surface micromachined bolometer-type thermal probe," *J. Vac. Sci. Technol. B*, 18(6), pp. 3600-3, 2000

[Li01] M.-H.Li, J.J.Wu, Y.B.Gianchandani, "Surface micromachined polyimide scanning thermocouple probes," *J. Microelectromech. Sys.*, 10(1), pp. 3-9, 2001

[Li02] M.-H.Li, J.-H.Lee, F.Cerrina, A.K.Menon, Y.B.Gianchandani, "Chemical and biological diagnostics using fully insulated ultracompliant thermal probes," *Proceedings on Solid-State Sensor, Actuator, and Microsystems Conference*, Hilton Head Island, SC, 2002, pp. 235-8

[Ma99] A.Majumdar, "Scanning thermal microscopy," *Annu. Rev. Mater. Sci.*, 29, pp. 505-85, 1999

[Mo95] K.Mochizuki, K.Watanabe, "A linear resistance-to-frequency converter," *Proc., Instrumentation and Measurement Technology Conf. (IMTC)*, Waltham, MA, 1995, pp. 339-43.

[Oc96] L.E.Ocola, D.Fryer, P.Nealey, J.dePablo, F.Cerrina, S. Kämmer, "Latent image formation: Nanoscale topography and calorimetric measurements in chemically amplified resists," *J. Vac. Sci. Technol. B*, 14(6), pp. 3974-9, 1996

[Sa93] G.R.Sarma, "Analysis of a constant voltage anemometer circuit," *Proc., Instrumentation and Measurement Technology Conf. (IMTC)*, Waltham, MA, 1993, pp. 731-6.

[Ve00] P.Vettiger, et al., "The "Millipede"-More than one thousand tips for future AFM data storage," *IBM J. Res. Develop.*, 44(3), pp. 323-40, 2000

[Yo00] D.J.Yonce, P.P.Bey Jr., T.L.J.Fare, "A DC autonulling bridge for real-time resistance measurement," *Trans. Circuits & Systems*, 47(3), pp. 273-7, 2000

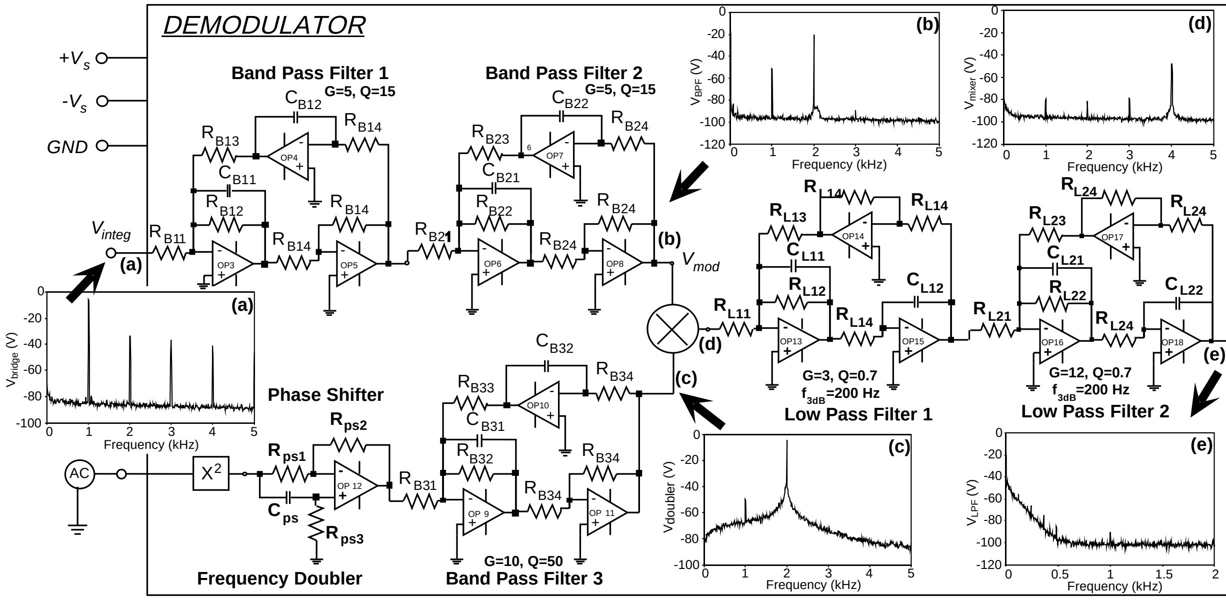

Fig. 3: Demodulator section of the interface circuit in Fig. 1. Embedded frequency spectra were obtained while scanning a real sample, not in a test mode. The scan results are present in Fig. 5.

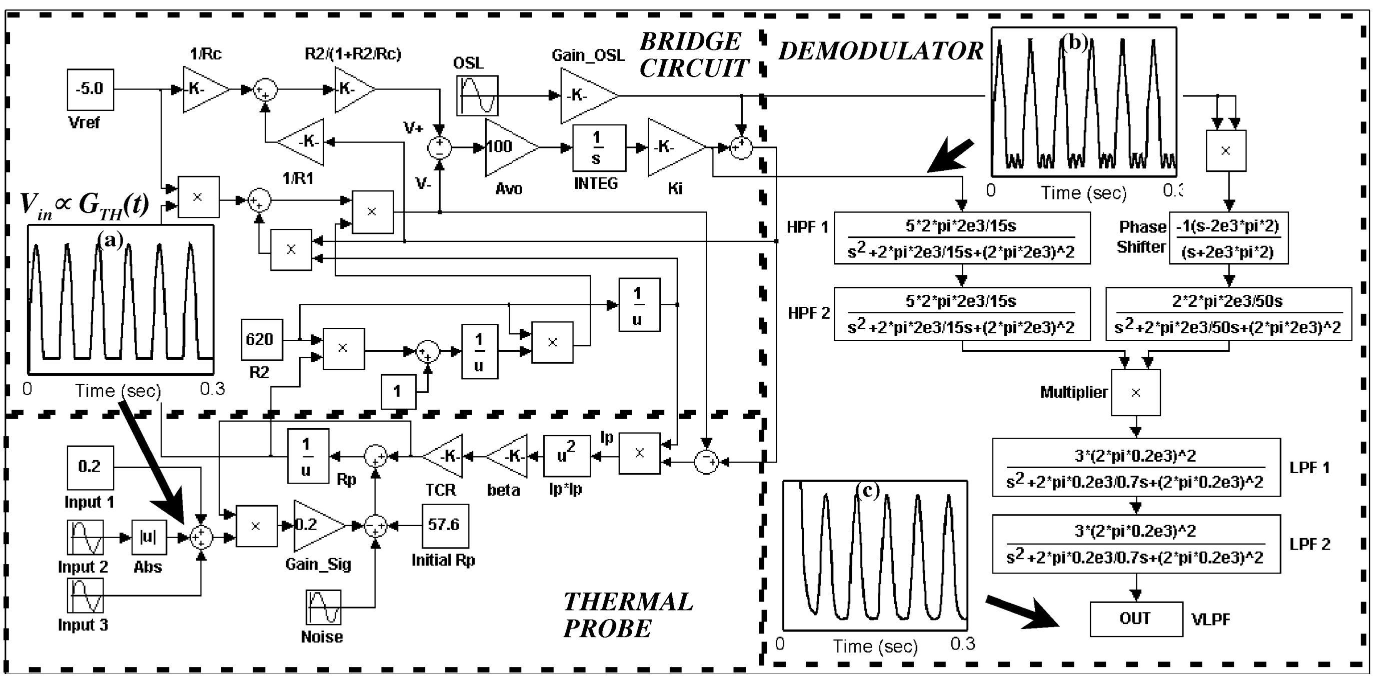

Fig. 4: State diagram for the scanning thermal microscopy system including thermal response of the probe and the electrical behavior of the circuit. The MatLab™ Simulink tool is used to optimize the circuit and evaluate overall performance, including noise immunity.

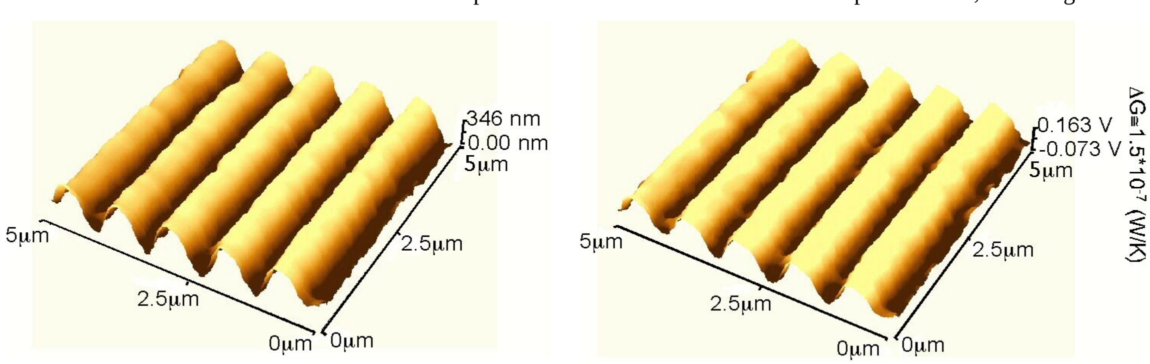

Fig. 5: Topographic (left) and thermal (right) images of developed 350 nm thick UV6™ photoresist scanned at 45°C tip temperature.